Monte Carlo study of a mixed spin-3/2 and spin-1/2 Ising ferrimagnetic model

G. M. Buendía and R. Cardona*
Departamento de Física, Universidad Simón Bolívar, Apartado 89000, Caracas 1080, Venezuela
(Received 14 July 1998; revised manuscript received 6 October 1998)

The magnetic properties of a mixed Ising ferrimagnetic model on a square lattice, in which the two interpenetrating square sublattices have spins that can take two values, $\sigma = \pm 1/2$, alternated with spins that can take four values, $S = \pm 3/2, \pm 1/2$, are studied. This model can be relevant for understanding the magnetic behavior of the new class of organometallic ferrimagnetic materials that exhibit spontaneous magnetic moments at room temperature. We carried out exact ground-state calculations for the model and employ a Monte Carlo algorithm to obtain the finite-temperature phase diagram for both the transition and compensation temperatures. The role of the different interactions in the Hamiltonian is explored. When only the nearest-neighbor interaction and the crystal-field term are included our results indicate no compensation point at finite temperature. When the next-nearest-neighbor interaction between the spins $\sigma = \pm 1/2$ exceeds a minimum value that depends on the other parameters in the Hamiltonian, a compensation point appears. The interaction between the $S = \pm 3/2$ spins, next-nearest neighbors in the lattice, has the effect of changing the compensation temperature. [S0163-1829(99)03905-3]

I. INTRODUCTION

Although theoretical models of ferrimagnetic systems have been around since the times of Néel,[1] there is recent experimental motivation for reopening this area of research. In recent years several groups have started an ambitious program to design and synthesize new classes of magnetic materials using the techniques of molecular organic chemistry. The goal is to produce organic materials soluble in organic solvents, biocompatible, optically transparent, with spontaneous moments at room temperature.[2] Ferrimagnetic ordering seems to play a fundamental role in these materials. The recently developed amorphous $V(TCNE)_{x \cdot y}$ (solvent), where TCNE is tetracyanoethylene, are organometallic compounds that, although they have not yet been crystallized, seem to have a 1/2-3/2 ferrimagnetic structure and ordering temperatures as high as 400 K.[3,4]

Mixed Ising systems have been introduced as simple models that can show ferrimagnetic behavior and that may show compensation points or *N*-type behavior in Néel classification nomenclature. The compensation point is the temperature where the resultant magnetization vanishes below the critical point. The existence of compensation temperatures has interesting applications, particularly in magneto-optic recording. Since this type of recording is done using the thermal effect of light, it is desirable that the magnetic field required for recording should change greatly in a relatively narrow temperature range, the precise effect that happens at the compensation point, where only a small driving field is required to reverse the magnetization. Also, the coercive force increases near the compensation temperature favoring the creation of small, stable, magnetic domains.[5] Mixed Ising models have been studied by several methods such as high-temperature series expansion,[6] and mean and effective-field approaches.[7,8] An exact solution of a mixed 1-1/2 Ising model on a Union Jack lattice has been found for a low-dimensional manifold in the parameter space.[9] A mixed Ising 3/2-1/2 model with nearest-neighbors and crystal-field interactions has shown interesting types of magnetic behavior, quite different from those of the 1-1/2 model, when studied using effective-field theories,[7] but so far this simple model has shown no compensation points. Recent studies using nonperturbative algorithms like Monte Carlo and transfer-matrix calculations for mixed $\pm 1/2$ and ± 2, $\pm 1,0$ spins have yielded important information on how compensation temperatures occur.[10,11] In order to obtain more reliable results and further understand the appearance of compensation points we study the mixed 3/2-1/2 Ising model with a more general Hamiltonian than the one studied with effective mean-field theories and with a nonperturbative technique, the Monte Carlo algorithm.

The aspects of interest in our study will be mainly the finite-temperature phase diagram and the possible existence of compensation points (which occurs in *N*-type ferrimagnets as classified in Ref. 1).

II. THE MODEL AND ITS GROUND STATES

The Hamiltonian we study includes nearest- and next-nearest-neighbors interactions and the crystal field. It has the form

$$\mathcal{H} = -J_1 \sum_{\langle nn \rangle} S_i \sigma_j - J_2 \sum_{\langle nnn \rangle} \sigma_m \sigma_n - J_3 \sum_{\langle nnn \rangle} S_i S_l - D \sum_i S_i^2 , \tag{1}$$

where $\sigma = \pm 1/2, S = \pm 3/2, \pm 1/2$. J_1, J_2, and J_3 are the exchange-interaction parameters and D is the crystal field, all in energy units, $\langle nn \rangle$ and $\langle nnn \rangle$ stand for nearest and next-nearest neighbors, respectively. Previous studies with effective mean-field theories only included the J_1 and the D terms.[7]

The models to be considered will be labeled by enumerating the parameters different from zero in the Hamiltonian. For example, the J_1-D model is the one in which all the parameters are zero except J_1 and D.

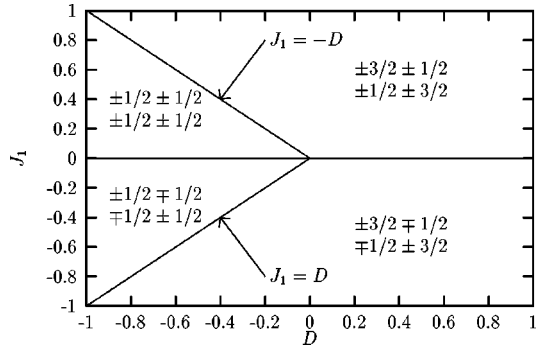

FIG. 1. Ground-state diagram for the J_1-D model. In each region the configurations of the 2×2 cells are indicated. J_1 and D are in energy units.

In order to obtain the ground-state diagram, we calculate the configurations of a 2×2 cell.[12] With rotational symmetry taken into account this cell has 40 different configurations. Which one is the ground state depends on the particular set of parameters in the Hamiltonian. As an example, in Figs. 1 and 2 we show the ground-state diagrams for the J_1-D and the J_1-J_2-D models, respectively. In each graph the ground-state configurations of the 2×2 cells are indicated. The equations of the boundaries between the regions are obtained by pairwise equating the ground-state energies. For the J_1-D model, Fig. 1, there are two possible ground states for the ferrimagnetic system ($J_1<0$) and two for the ferromagnetic system ($J_1>0$). For the J_1-J_2-D model with $J_1<0$ the ground-state diagram is divided in four regions, as seen in Fig. 2.

III. MONTE CARLO CALCULATIONS

We have applied standard importance sampling methods to simulate the Hamiltonian given by Eq. (1). Periodic boundary conditions on $L\times L$ lattices were imposed and configurations were generated by sequentially traversing the lattice and making single-spin flip attempts. The flips are accepted or rejected according to a heat-bath algorithm. Our data were generated with 10^4 Monte Carlo steps per spin in lattices with $L=40$, after 10^3 warming steps per spin. The error bars were taken from the standard deviation of blocks of 10^2 measurements each. We define $\beta=1/k_BT$ and take

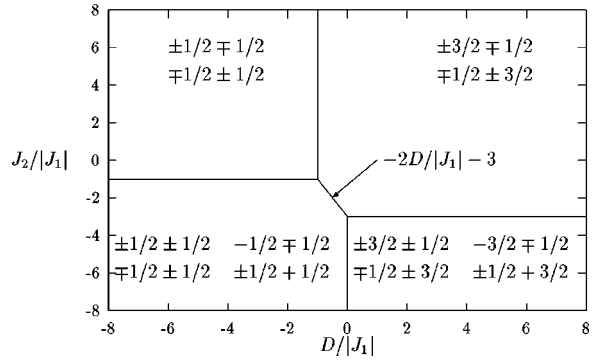

FIG. 2. Ground-state diagram for the J_1-J_2-D model with $J_1<0$. There are four regions, in each of which the configurations of the 2×2 cells are indicated.

Boltzmann's constant $k_B=1$. Our program calculates the internal energy per site,

$$E=\frac{1}{L^2}\langle H\rangle, \tag{2}$$

the specific heat per site,

$$C=\frac{\beta^2}{L^2}[\langle H^2\rangle-\langle H\rangle^2], \tag{3}$$

the sublattice magnetizations per site,

$$M_1=\frac{2}{L^2}\left\langle \sum_i S_i \right\rangle, \quad M_2=\frac{2}{L^2}\left\langle \sum_j \sigma_j \right\rangle, \tag{4}$$

the total magnetization per site, $M=(M_1+M_2)/2$, and the susceptibility,

$$\chi=\beta(\langle M^2\rangle-\langle M\rangle^2). \tag{5}$$

Since we are particularly interested in studying the possible existence of compensation points, all our numerical results are obtained for the ferrimagnetic case $J_1<0$.

In order to locate the compensation points an order parameter per spin defined by

$$O=\frac{1}{L^2}\left\langle \left| \sum_{i,j} S_i+\sigma_j \right| \right\rangle, \tag{6}$$

which is equivalent to the average of the absolute value of the total magnetization, was also measured. At the compensation temperature T_{comp}, the total magnetization of the system must be zero and, in the case of an infinite lattice, the order parameter O would reach the zero value. For finite lattices, the order parameter O reaches an absolute minimum at the compensation temperature. Another efficient way to locate T_{comp} is to find the temperature at which the sublattice magnetizations have equal magnitude and opposite signs [$|M_1|=|M_2|$ and $\mathrm{sgn}(M_1)=-\mathrm{sgn}(M_2)$ at T_{comp}], such that the total magnetization is zero.

IV. RESULTS

A. The J_1-D model

The results for the order parameter shown in Fig. 3 indicate that this model has no compensation point. From these results we can distinguish three types of magnetic behavior. When $D/|J_1|\geqslant 0$ the magnetization curves are of type Q in the Néel classification,[1] typical of a ferromagnet. As $D/|J_1|$ becomes negative, in the range $-1<D/|J_1|<0$, the magnetization falls rapidly from its saturation value at $T=0$ in a way that is not described in Néel's classification. At $D/|J_1|=-1$ there is a mixed phase at $T=0$ where two ground-state configurations occur with equal probability, the ground state of the S spins consists of a mixed phase in which they can take the values $S=\pm1/2$ or $S=\pm3/2$ with equal probability (see Fig. 1). Hence the ground-state magnetization of the system is equal to the average of the magnetizations of the two phases. For $D/|J_1|<-1$, the magnetization becomes type L (in Néel's classification). Plots of the sublattice mag-

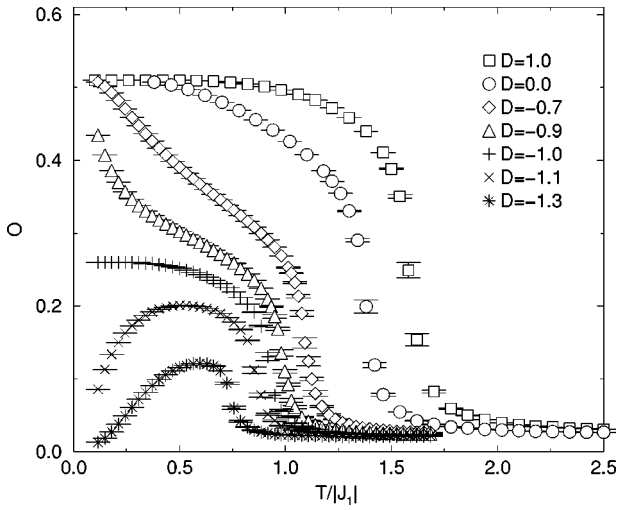

FIG. 3. Order parameter vs temperature for the J_1-D model for several values of $D/|J_1|(J_1=-1)$.

netizations show that the S sublattice is the one with the strongest dependence on the parameter D, as can be seen in Fig. 4.

Figure 5 shows the specific-heat curves. Notice that when $D/|J_1|\rightarrow -1$ there is a secondary peak in the curves that increases and moves toward zero temperatures as $D/|J_1|$ approaches -1. Also, if two curves have a parameter value $D/|J_1|=-1\pm\Delta$, then the low-temperature behavior of the curves is the same. This suggests that the existence of the mixed phase at $D/|J_1|=-1$ induces a phase transition at $T=0$, such that the system has a zero-temperature phase transition as well as a finite-temperature one at $T_{crit}/|J_1|=0.92\pm0.01$. The symmetry of the heat capacity with respect to $D/|J_1|+1$ is a rather common phenomenon at field-driven first-order transitions, even for systems that only have a phase transition at $T=0$, such as the one-dimensional Ising chain. At $T=0$ the specific heat vanishes, due the finite energy gap between the ground state and the lowest excited state. For an example in a lattice-gas system, see, e.g., (Ref. 13).

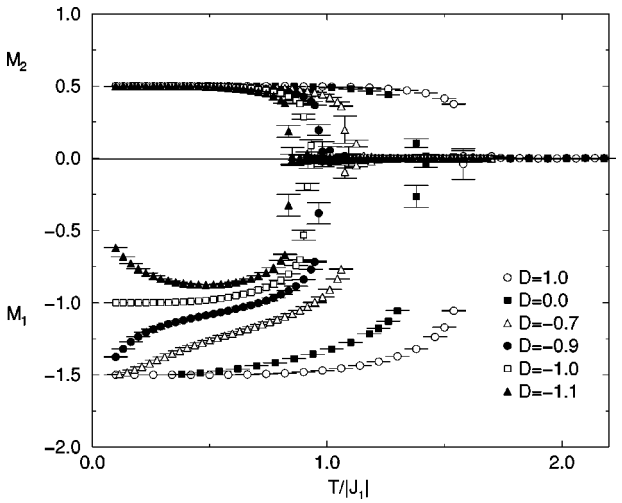

FIG. 4. Temperature dependence of the sublattice magnetizations M_1 and M_2 for the J_1-D model for several values of $D/|J_1|(J_1=-1)$. As can be verified in Fig. 3 they never cancel each other and both go to zero at the critical temperature.

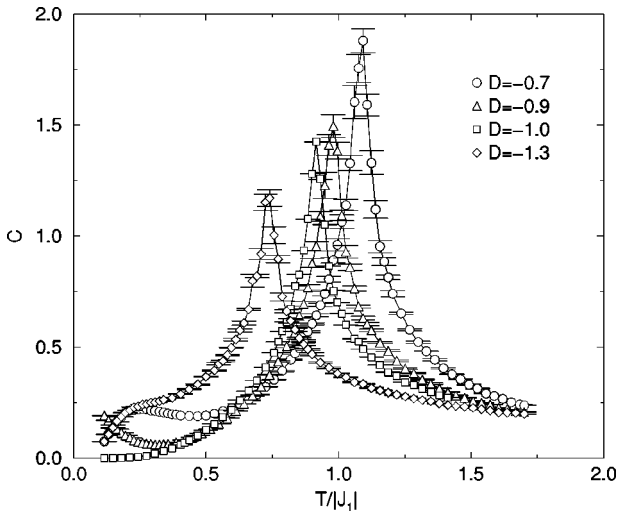

FIG. 5. Specific heat vs temperature for the J_1-D model for several values of $D/|J_1|$ $(J_1=-1)$. The position of the maximum gives an estimate of the T_{crit}. The lines are guides for the eye.

The zero-temperature phase transition can also be seen in the magnetic susceptibility curves. In Fig. 6 the plots of the inverse susceptibility $1/\chi$ show the critical temperatures defined by the value at which $1/\chi\rightarrow 0$. Notice that when $D/|J_1|=-1$ the inverse susceptibility goes to zero at the critical temperature $T_{crit}/|J_1|=0.92\pm0.01$, and also at $T=0$. For values of $D/|J_1|$ near -1, the inverse susceptibilities present anomalous local minima at low temperatures due to its proximity to the mixed phase at $T=0$.

In Fig. 7 we present the critical temperatures calculated from the maxima in the susceptibilities and previous results obtained with an effective-field approximation.[7] When $D\rightarrow -\infty$, the J_1-D model becomes a standard $\pm1/2$ Ising system with a critical temperature (predicted from Onsager's solution) $T_{crit}(\text{exact})/|J_1|\approx0.575$. In the limit $D\rightarrow\infty$ the model becomes a standard Ising model with half the spins taking the values $\pm1/2$ and the other half taking the values $\pm3/2$, with a critical temperature $T_{crit}(\text{exact})/|J_1|\approx1.725$. Figure 7

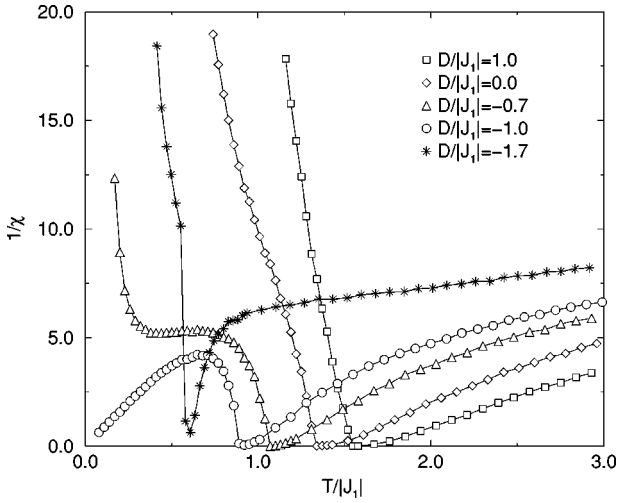

FIG. 6. Temperature variation of the inverse magnetic susceptibilities for several values of $D/|J_1|$ for the J_1-D model. The minimum gives an estimate of the T_{crit} that is consistent with the one obtained from Fig. 5. The lines are guides for the eye.

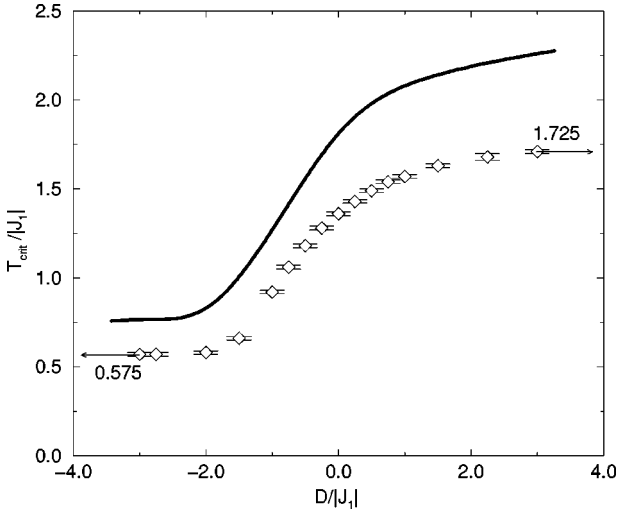

FIG. 7. The finite-temperature phase diagram for the J_1-D model. The Monte Carlo results are indicated by the $\diamond$ with error estimates. The solid line corresponds to effective-field results (Ref. 7). The arrows indicate the exact value of T_{crit} in the two limiting cases, $D/|J_1| = \pm\infty$.

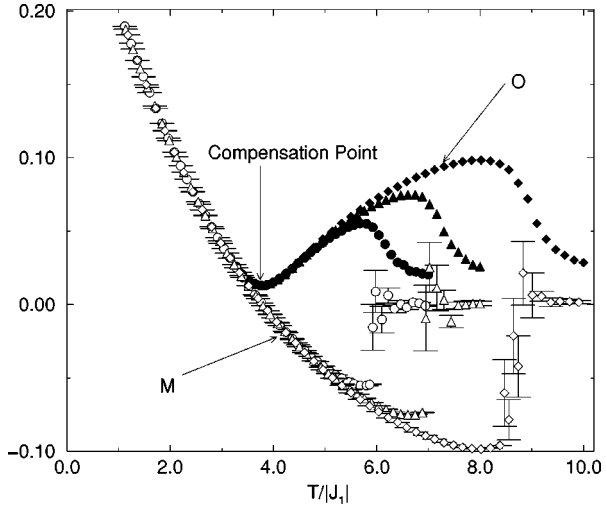

FIG. 8. The total magnetization and the order parameter vs the temperature for the J_1-J_2-D model at $D/|J_1| = -1$ and $J_2/|J_1| = 10$ ($\bigcirc$), $J_2/|J_1| = 12$ ($\triangle$), and $J_2/|J_1| = 15$ ($\diamond$). The empty symbols are for the total magnetization and the equivalent filled symbols correspond to the order parameter. Notice that the compensation temperature is nearly independent of the value of $J_2/|J_1|$ (if $J_2 > J_2^{min}$) but the critical temperature increases with increasing values of $J_2/|J_1|$.

shows that our results are consistent with the exact solutions in both limiting cases. Notice that the critical temperature shows no special behavior at $D/|J_1| = -1$, which corresponds to a phase transition in the ground-state diagram (Fig. 1). The reason is the absence of next-nearest interactions J_3, so that the system of S spins can be considered as a noninteracting system at low T. For a detailed discussion of this kind of ''cage effect'' for an $S=1$ antiferromagnet, see Ref. 14.

B. Effect of next-nearest-neighbors interactions: J_1-J_2-J_3-D model

Since our data show that the J_1-D model does not have compensation points and there are recent results that indicate that some mixed Ising ferrimagnetic models present compensation points when the next-nearest-neighbors interaction between the σ spins (J_2) is taken into account;[10,11] we include the J_2 term in the Hamiltonian, i.e., the J_1-J_2-D model. The total magnetization curves shown in Fig. 8 clearly indicate the presence of compensation temperatures for this model. In the same figure we also present the order-parameter curves and show that they reach an absolute minimum at the compensation point. Notice that, for a fixed value of $D/|J_1|$, the compensation temperature remains basically unchanged once $J_2/|J_1|$ exceeds a minimum value; however, as expected, the critical temperature keeps increasing with increasing values of J_2. These results are quite general and do not depend on the particular value of $D/|J_1|$ selected in Fig. 8.

In order to understand how the compensation phenomenon occurs we present the absolute values of the sublattice magnetizations in Fig. 9. As the $J_2/|J_1|$ parameter increases, the ferromagnetic interaction between the σ spins grows, enabling the σ sublattice (M_2) to remain ordered at higher temperatures. At the same time, the S sublattice magnetization (M_1) decreases with increasing temperatures until both sublattices magnetizations are equal in magnitude at some temperature below the critical one. Since the sublattices magnetizations have opposite signs at this temperature the compensation point occurs. Further increase of $J_2/|J_1|$ does not change the compensation temperature that has already been reached, but has the effect of keeping the system ordered at higher temperatures such that the critical point occurs at higher temperatures.

We have plotted the critical and compensation temperatures as a function of $J_2/|J_1|$ for several values of $D/|J_1|$ as shown in Fig. 10. These plots clearly show that the compensation temperatures do not appear until the J_2 interaction takes some minimum value that depends on $D/|J_1|$, after which T_{comp} is almost independent of J_2. It can also be seen that as $J_2/|J_1|$ grows the variation of the critical temperature becomes independent of the crystal-field parameter D.

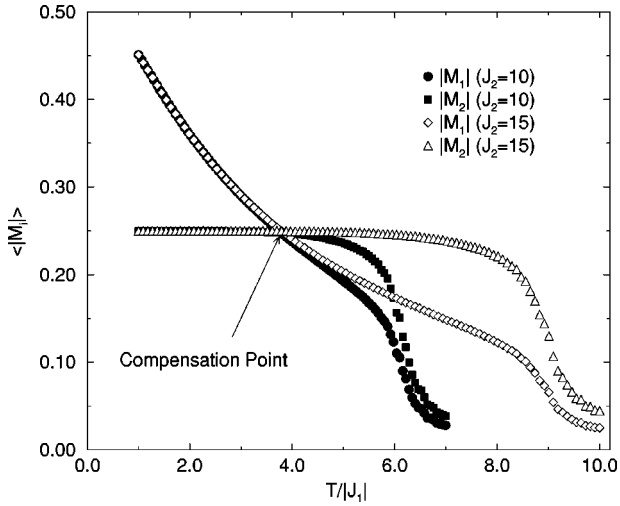

FIG. 9. Absolute value of the sublattice magnetizations vs the temperature for the J_1-J_2-D model at $D/|J_1| = -1$ and $J_2/|J_1| = 10,15$. The compensation temperature is reached at the crossing point $|M_1(T_{comp})| = |M_2(T_{comp})|$, where the total magnetization is zero and the order parameter has a minimum as seen in Fig. 8.

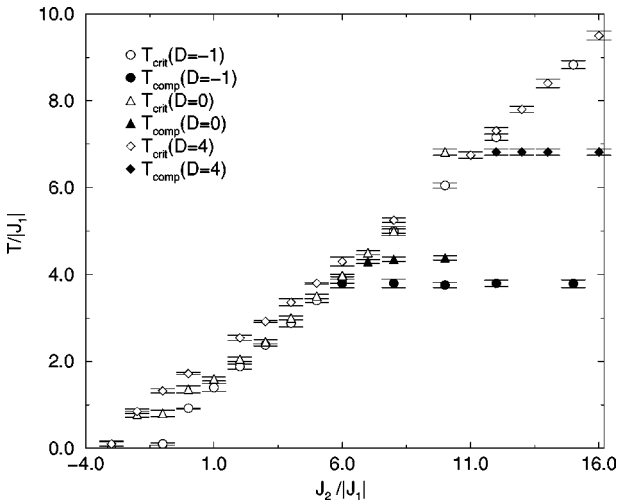

FIG. 10. Critical and compensation temperatures as function of $J_2/|J_1|$ for the J_1-J_2-D model at $D/|J_1|=-1,0,4$. The minimum value of $J_2/|J_1|$ for the compensation temperature to appear depends on the value of $D/|J_1|$.

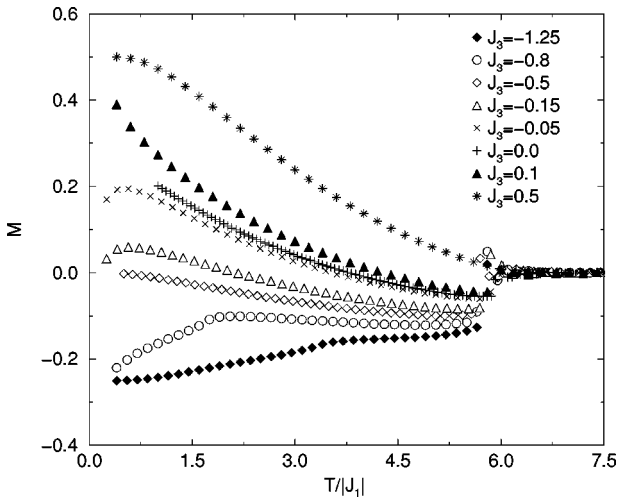

FIG. 11. Total magnetization vs temperature for the J_1-J_2-J_3-D model at $D/|J_1|=-1$ and $J_2/|J_1|=10$, for several values of $J_3/|J_1|$. For this choice of parameters the compensation point only exists if $-0.5<J_3/|J_1|<0.5$.

We have also found compensation points when the next-nearest-neighbor interaction between the S spins (J_3) is included in the Hamiltonian, the J_1-J_2-J_3-D model. In Fig. 11 we show the total magnetization curves for different values of $J_3/|J_1|$ with fixed $D/|J_1|$ and a value of $J_2/|J_1|$ above the minimum required in order to obtain a compensation point. As Fig. 11 shows, the compensation temperature increases toward the critical temperature with increasing positive values of $J_3/|J_1|$. When, for a big enough value of $J_3/|J_1|$, both temperatures become equal we do not have a compensation point anymore, only a critical point. For increasing negative values of $J_3/|J_1|$ the compensation temperature decreases until it disappears. Consequently, small variations of $J_3/|J_1|$ can change the compensation point from zero up to the critical temperature, but have little effect on the critical point. The value of $J_3/|J_1|$ for which T_{comp} goes to zero corresponds to a phase transition in the ground-state diagram of the J_1-J_2-J_3-D model. All our results are for a 40×40 system size, but since the compensation point is not a critical point, a study of finite-size effects would add little to its analysis.

V. CONCLUSIONS

We have applied a Monte Carlo algorithm to study a mixed Ising system on a square lattice. Our model has two interpenetrating square sublattices, one of spins $\sigma=\pm1/2$ and the other with spins $S=\pm3/2$. The Hamiltonian includes nearest-, next-nearest-neighbors interactions and the crystal field. In order to study the ferrimagnetic ordering the coupling between nearest neighbors is chosen to be antiferromagnetic. We have calculated the exact ground-state energies and the finite-temperature phase diagram showing the critical and compensation temperatures.

For the J_1-D model (the model with only nearest neighbors and the crystal field) we obtained a critical temperature dependence with the $D/|J_1|$ parameter that is similar to the one obtained through effective-field theory for the same model.[7] Our Monte Carlo results are consistent with Onsager's exact solutions in the two limiting cases, and thus superior to the effective-field result. We have also found a magnetization curve type that is not described in Néel classification.[1] The data show that the J_1-D model does not have compensation points. This is consistent with previous nonperturbative results in similar models.[10,11]

Our results show that a compensation point appears when the next-nearest-neighbors interaction between the σ spins (J_2) is included in the Hamiltonian. The minimum value of $J_2/|J_1|$ for a compensation point to exist depends on the value of the other parameters in the Hamiltonian. We found that for the J_1-J_2-D model once the compensation point appears it remains approximately constant for any $J_2\geqslant J_2^{min}$ for a fixed value of $D/|J_1|$.

The effect of the next-nearest-neighbor interaction J_3 between the S spins, the J_1-J_2-J_3-D model, is to change the compensation temperature in a range that varies from zero up to the critical temperature.

Our study suggests that compensation temperatures are extremely dependent on the interactions in the Hamiltonian and that there is a relatively narrow combination of parameters for which they can exist. Experimental evidence of the effect of long-range interactions on compensation points has already been found.[15,16]

ACKNOWLEDGMENTS

We are indebted to Mark Novotny and Erik Machado for many useful comments during the course of this work.

*Present address: Geophysics Department, Stanford University, Stanford, CA 94305.

[1] L. Néel, Ann. Phys. (N.Y.) **3**, 137 (1948).

[2] *Proceedings of the Conference on Ferromagnetic and High Spin Molecular-Based Materials*, edited by H. Iwamura and J. S. Miller [Mol. Cryst. Liq. Cryst. Sci. Technol., Sect. A **232** (1993)]; *Magnetic Molecular Materials*, Vol. 198 of *NATO Advanced Study Institute, Series B: Physics*, edited by D. Gatteschi,

O. Kahn, J. S. Miller, and F. Palacio (Kluwer Academic, Dordrecht, 1991).

[3] J. M. Manriquez, G. T. Yee, R. S. McLean, A. J. Epstein, and J. S. Miller, Science **252**, 1415 (1991); G. Du, J. Joo, and A. Epstein, J. Appl. Phys. **73**, 6566 (1993).

[4] B. G. Morin, P. Zhou, C. Hahm, and J. A. Epstein, J. Appl. Phys. **73**, 5648 (1991).

[5] N. V. Mushnikov, N. K. Zajkov, and V. S. Gaviko, J. Alloys Compd. **191**, 63 (1993); N. Inamura, in *Physics and Engineering Applications of Magnetism*, edited by Y. Ishikawa and N. Miura (Springer-Verlag, Berlin, 1991).

[6] G. Hunter, R. Jenkins, and C. J. Tinsley, J. Phys. A **23**, 4547 (1990); R. G. Bowers and B. Y. Yousif, Phys. Lett. **96A**, 49 (1983).

[7] T. Kaneyoshi, M. Jascur, and P. Tomczak, J. Phys.: Condens. Matter **4**, L653 (1992); **5**, 5331 (1993).

[8] N. Benayad, A. Dakhama, A. Klumper, and J. Zittartz, Ann. Phys. (Leipzig) **5**, 387 (1996).

[9] A. Lipowski and T. Horiguchi, J. Phys. A **29**, L261 (1995).

[10] G. M. Buendía and M. A. Novotny, J. Phys.: Condens. Matter **9**, 5951 (1997); G. M. Buendía, M. A. Novotny, and J. Zhang, in *Computer Simulation Studies in Condensed Matter Physics VII*, edited by D. P. Landau, K. K. Mon, and H. B. Schuttler (Springer-Verlag, Berlin, 1994).

[11] G. M. Buendía and J. A. Liendo, J. Phys.: Condens. Matter **9**, 5439 (1997); G. M. Buendía and M. A. Novotny, J. Phys. IV **7**, C1-175 (1997).

[12] G. Karl, Phys. Rev. B **7**, 2050 (1973); M. Schick, Prog. Surf. Sci. **11**, 245 (1982).

[13] P. A. Rikvold, M. A. Novotny, and T. Aukrust, Phys. Rev. B **43**, 202 (1991).

[14] P. A. Rikvold, J. B. Collins, G. D. Hansen, and J. D. Gunton, Surf. Sci. **203**, 500 (1988); J. B. Collins, P. A. Rikvold, and E. T. Gawlinski, Phys. Rev. B **38**, 6741 (1988); P. A. Rikvold and J. D. Gunton, Surf. Sci. **221**, 277 (1989).

[15] L. Ertl, G. Endl, and H. Hoffmann, J. Magn. Magn. Mater. **113**, 227 (1992).

[16] Eric E. Fullerton, J. S. Jiang, Christine Rehm, C. H. Sowers, S. D. Bader, J. B. Patel, and X. Z. Wu, Appl. Phys. Lett. **71**, 1579 (1997).